EPSC Abstracts
Vol. 6, EPSC-DPS2011-563-1, 2011
EPSC-DPS Joint Meeting 2011
© Author(s) 2011

On the survival of an internal liquid water reservoir at Enceladus' south pole

M. Běhounková (1), G. Tobie (2), G. Choblet (2) and O. Čadek (1)
(1) Charles University in Prague, Faculty of Mathematics and Physics, Department of Geophysics, Czech Republic
(2) Université de Nantes, CNRS, Laboratoire de Planétologie et Géodynamique de Nantes, UMR 6112, France
(marie.behounkova@mff.cuni.cz)

Abstract

The eruptions of water vapor and ice particles on Enceladus' south pole [1] together with huge heat production reaching $15 - 21\,\mathrm{GW}$ [2] suggest the presence of a strong source of energy within Enceladus' interior. Tidal dissipation is the most likely candidate. Nevertheless, the significant power can be reproduced only if a liquid layer exists at depth [3]. As the presence of a global ocean is challenging [4, 3], we suppose here only a local ocean at the base of the ice shell. By systematically varying the orbital parameters and width of a local ocean, we investigate the conditions under which a liquid reservoir can be thermally stable in Enceladus'interior, see also [5].

1. Method and model

By varying orbital and physical properties, specifically the eccentricity and the predefined width Δ of the local liquid reservoir below the ice I shell, we study whether the liquid reservoir may be maintained and what is the minimal thickness of such a predefined reservoir in order to avoid its crystallization. In order to assess the thermal stability of the liquid reservoir and its effect on the dynamics of the overlying ice shell, we use a tool that solves simultaneously subsolidus convection and tidal dissipation in 3D spherical shell [6]. In this approach, tidal dissipation induced by the presence of external tide-generating body is taken as a source of volumetric energy for the convection [6]. Numerically, the reservoir at the base of the icy shell is represented by the following boundary conditions: free-slip and constant (melting) temperature are imposed in the convective part, the force equilibrium is prescribed for the tidal dissipation part. For areas with no liquid reservoir, no-slip and constant heat flux corresponding to the radiogenic heating in the core is prescribed. By balancing the melt production and the heat transported from the liquid reservoir, the conditions for possible survival of such a reservoir are predicted.

Two end-member models are considered for the description of melt production and transport: First, the instantaneous melt extraction (IME model) is employed, i.e. any melt produced in a given time step is immediately transported to the base of the icy shell, without interacting with the underlying ice. Second, thermal equilibrium percolation (TEP model) is supposed. In this approach, any created melt is propagated downwards and a thermal equilibrium is taken into account, i.e. latent heat due to melting or freezing is always balanced by temperature variations of the surrounding ice.

The rheological properties of viscosity are described by the Arrhenius law. The activation energy is $50\,\mathrm{kJ/mol}$ for temperatures lower than $255\,\mathrm{K}$ and $E^* = 190\,\mathrm{kJ/mol}$ for temperatures higher than $255\,\mathrm{K}$, in order to take into account creep enhancement due to premelting effect. The reference viscosity η_{ref} is $10^{15}\,\mathrm{Pa}\cdot\mathrm{s}$ for the reference temperature T_{ref} $255\,\mathrm{K}$.

2. Results

All simulations presented here are started from a statistical steady state (thermal equilibrium state) without any tidal dissipation, i.e. for zero eccentricity. Then the eccentricity is increased to a particular value varying between 1 and 10 times the current eccentricity e_c.

2.1. Influence of eccentricity

The results for the internal reservoir covering the whole southern hemisphere ($\Delta = 180°$) are shown in Figs. 1–2 for eccentricities 4-, 5- and 6-times higher than the current eccentricity. Due to significant tidal dissipation, the interior temperature within the convecting part increases progressively. The global dissipation first slightly increases until the internal temperature reaches the value corresponding to the maximum heat production ($T_{\max} = 263\,\mathrm{K}$, for the rheological parameters chosen here), then the global dissipation

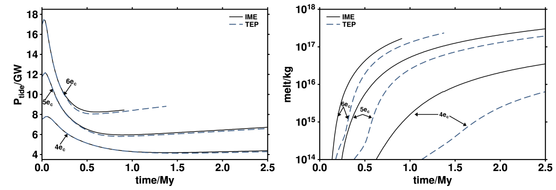

Figure 1: Time evolution of global tidal heating (left) and melt production (right), for ocean width 180 °.

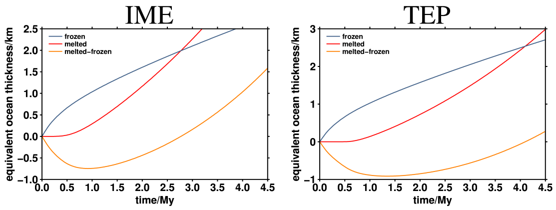

Figure 2: Variations of ocean thickness (orange) due to tidally-induced internal melting (red) and water solidification due to heat loss at the ocean/ice interface (blue) for the model with ocean width 180 ° and 5-times current eccentricity.

strongly decreases as the internal temperature is growing fast. At later stages, a slight increase of the dissipation is observed due to heating of the cold areas in the vicinity of the convecting part (Fig. 1a). Additionally, only weak dependence of the global dissipation on the melt model is observed. The melt production (Fig. 1b) occurs predominantly below the stagnant lid and it depends strongly on the global dissipation. Also, as expected, the melt production for TEP model is delayed due to the interaction with ice in comparison with the most efficient model of the melt production (IME model).

Fig. 2 displays the net variations of ocean thickness (orange) corresponding to the difference between water production due to tidally-induced internal melting (red) and water solidification due to heat loss at the ocean/ice interface (blue). At the beginnning of the simulations (Fig. 2, 5x e_c), the ocean first crystallizes, but after 3 My in IME model and 4 Myr in TEP model, the internal melt production balances the interface freezing and the ocean thickness rapidly increases. For eccentricity of $4e_c$, increase of the ocean thickness is also obtained but after a longer initial freezing phase.

2.2. Influence of reservoir width

The global tidal heating production for the initial conditions and for different reservoir widths is summarized in Tab. 1. Similarly to Tobie et al. [3], the width of the reservoir must be spread over majority of the southern hemisphere in order to obtain high deformations connected to the high tidal dissipation producing the melt. In the case of width $\Delta = 60°$, the eccen-

e/e_c	$\Delta = 60°$	$\Delta = 120°$	$\Delta = 180°$
1	0.003	0.09	0.5
3	0.023	0.81	4.3
6	0.090	3.24	17.2
10	0.250	9.00	47.5

Table 1: The global tidal dissipation in GW for equilibrium initial conditions depending on eccentricity and width of the liquid reservoir.

tricity must be an order magnitude higher than the current one. For widths 120° and 180°, we have obtained melting for eccentricities higher than $5e_c$ and $3e_c$, respectively.

3. Summary and Conclusions

In our models, melt production is predicted for the liquid reservoir covering 120° and 180° area around the south pole for eccentricities higher than $5e_c$ and $3e_c$, respectively. For the reservoir width $\Delta = 60°$, the tidal dissipation rate is negligible unless the eccentricity is one order of magnitude higher than the current one. For $\Delta = 180°$, tidally-induced internal melting is able to balance the freezing due to convective heat loss for eccentricity larger than 4 times the current value of 0.0045. These results suggest that the survival of an internal liquid reservoir is possible if Enceladus experiences frequent periods with elevated orbital eccentricity during its evolution. An ocean may survive if periods with low eccentricity (close to the current value) last only a few millions of years. However, if the liquid zone gets too small ($< 120°$), it becomes difficult to restart the melting process.

Acknowledgements

This work was supported by the CSF project No. P210/10/P306, MSM0021620860 of the Ministry of Education of the Czech Republic, Czech-French MOBILITY project Barrande (MEB021129). The research leading to these results has received funding from the European Research Council under the European Community's Seventh Framework Programme (FP7/2007-2013 Grant Agreement no. 259285).

References

[1] C.C. Porco et al. *Science*, 311, 1393, 2006.

[2] J.R. Spencer et al., *EGU General Assembly*, 12:EGU2010–12207, 2010.

[3] G. Tobie et al., *Icarus*, 196:642–652, 2008.

[4] Roberts and Nimmo, *Icarus*, 194:675–689, 2008.

[5] G. Tobie et al., *EPSC abstract*, 2011.

[6] M. Běhounková et al., *J. Geophys. Res.*, 115, E09011, 2010.